

Orientation of C_{60} molecules in the $(3\sqrt{3}\times 3\sqrt{3})R30^\circ$ and $(\sqrt{13}\times\sqrt{13})R14^\circ$ phases of $C_{60}/\text{Ge}(111)$ single layers

Mattia Fanetti,¹ Luca Gavioli,¹ Cinzia Cepek,² and Massimo Sancrotti^{1,2}

¹*CNR-INFM and Dipartimento di Matematica e Fisica, Università Cattolica, via dei Musei 41, 25121 Brescia, Italy*

²*Laboratorio Nazionale TASC-CNR-INFM, SS 14, Km 163.5, 34012 Basovizza (TS), Italy*

(Received 11 September 2007; revised manuscript received 28 November 2007; published 14 February 2008)

The structure of the $(3\sqrt{3}\times 3\sqrt{3})R30^\circ$ and $(\sqrt{13}\times\sqrt{13})R14^\circ$ phases of $C_{60}/\text{Ge}(111)$ single layer has been studied by scanning tunneling microscopy. Submolecular resolution allows to distinguish differently oriented molecules. In the $(3\sqrt{3}\times 3\sqrt{3})R30^\circ$ phase, the molecules are arranged in rhomboidal groups of four molecules, named tetramers. The (2×2) periodicity in the domains of homogeneously oriented tetramers is due to the alternating orientation of the molecules within the tetramer, accounting for the observed $(3\sqrt{3}\times 3\sqrt{3})R30^\circ$ low energy electron diffraction pattern. The symmetry of the molecular lattice suggests that the molecules interact only with the first layer of substrate atoms. The orientation of each molecule is mainly determined by the configuration of the substrate atoms in the adsorption site, even though a contribution from the intermolecular interaction is likely present. In the $(\sqrt{13}\times\sqrt{13})R14^\circ$ phase, the observed submolecular features indicate that all the molecules have the same adsorption configuration, with a hexagon facing the substrate. The threefold symmetry of the molecular lattice suggests that the C_{60} -Ge interaction involves also the atoms of the second layer of the substrate.

DOI: [10.1103/PhysRevB.77.085420](https://doi.org/10.1103/PhysRevB.77.085420)

PACS number(s): 61.48.-c, 68.37.-d, 68.37.Ef, 68.55.-a

I. INTRODUCTION

The behavior of C_{60} molecules adsorbed on semiconductor surfaces and the properties of thin C_{60} films have attracted much interest in recent years (see, for example, Refs. 1–11). In fact, C_{60} monolayers on single crystal substrates represent a well ordered quasi-two-dimensional (2D) system with peculiar crystalline properties, which, in turn, are closely related to the electronic properties of the system (see, for example, Ref. 12). The transport properties and the electronic structure of a C_{60} thin film depend indeed on the interaction with the substrate and between the molecules, and their competition determines the geometric structure of the film and the molecule orientation as well.^{2,13–16} As a consequence, several studies are present in the literature devoted to investigating how the C_{60} molecules are oriented with respect to the substrate and how the orientational degrees of freedom play a role in the resulting periodicity and/or symmetry of the system.^{9,13–15,17–20}

The C_{60} adsorption on $\text{Ge}(111)$ - $c(2\times 8)$ surface has been studied by x-ray diffraction,⁷ low energy electron diffraction (LEED),^{1,8} scanning tunneling microscopy (STM),^{1,4,5} and spectroscopy techniques such as x-ray photoelectron spectroscopy and ultraviolet photoelectron spectroscopy (UPS).^{2,8} Two different ordered molecular configurations have been observed,¹ depending on the preparation temperature: the $(3\sqrt{3}\times 3\sqrt{3})R30^\circ$ phase and the $(\sqrt{13}\times\sqrt{13})R14^\circ$ phase, defined with respect to the $\text{Ge}(111)$ - (1×1) unit cell. The former is obtained by annealing (or depositing) a multilayer C_{60} film at 450–500 °C.¹ The latter is obtained by annealing (or depositing) a C_{60} multilayer at more than 500 °C,¹ up to the single layer desorption temperature, which on $\text{Ge}(111)$ is ~ 670 °C.⁸ After the annealing in this temperature range, only a single molecular layer is still present on the substrate because the layers above are desorbed from the surface at a temperature close to the sublimation temperature of bulk C_{60} in vacuum, which is ~ 230 °C.²¹

The $(3\sqrt{3}\times 3\sqrt{3})R30^\circ$ (R3 hereafter) LEED pattern corresponds to a hexagonal 2D superlattice with a periodicity of 2.08 nm. However, the STM images reveal a close packed hexagonal superlattice in which the molecule-molecule distance is ~ 1.0 nm,¹ i.e., the periodicity observed by STM is one-half that observed by LEED. Xu *et al.* explained this discrepancy by supposing that a reconstruction of $\text{Ge}(111)$ adatoms is responsible for the R3 LEED pattern.¹ In contrast, Goldoni *et al.* suggested that the observed R3 periodicity is due to an alternating orientation of the molecules.² In this model, which will be discussed in the next section, the different molecular orientations are determined by different substrate atom configurations in each adsorption site. This implies that the interaction between C_{60} and substrate is the predominant factor in the resulting molecular orientation. On the other hand, the short distance (1.02 nm) between neighboring molecules indicates that a role of the intermolecular interactions cannot be *a priori* excluded. For example, in the C_{60} molecular crystal, where the neighbor molecules are at the same distance of the system studied here, below -20 °C²² the intermolecular interactions are responsible for the orientation of the C_{60} . In any case, the question about the origin of the observed R3 LEED pattern on $\text{Ge}(111)$ is still open since direct observations of the molecular orientation in this phase are missing.

By heating the system above 500 °C, a phase transition occurs and the monolayer rearranges in the $(\sqrt{13}\times\sqrt{13})R14^\circ$ phase¹ (R13 hereafter). In this case, the molecular lattice observed by STM is a hexagonal lattice with a lower density with respect to the former (molecular lattice unit vector: 1.44 nm) and the observed R13 LEED pattern is consistent with the lattice periodicity observed by STM.¹ For this reason, no long-range extra periodicity due to the molecular orientation is expected in this case.

In this work, we present the results of LEED and STM investigations on the two mentioned phases of the C_{60} mono-

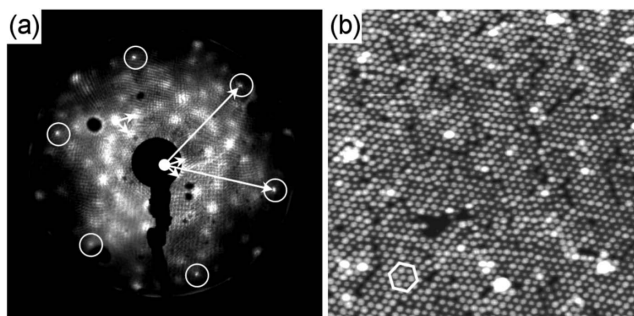


FIG. 1. (a) R3 LEED pattern ($E_p=33$ eV) of the C_{60}/Ge monolayer obtained by annealing a C_{60} multilayer at 450°C . The circles indicate the spots of the (1×1) substrate periodicity; the long arrows are the reciprocal unit vectors. The short arrows indicate the R3 reciprocal unit vectors. (b) STM image ($40\times 40\text{ nm}^2$, $V=-1.6$ V, $I=0.6$ nA) of the same system, where the submolecular features are not resolved. The white hexagon represents the hexagonal molecular network (first neighbor distance: ~ 1 nm).

layer on Ge(111) substrate. The analysis of STM images with submolecular resolution allows to disentangle different molecular orientations and to describe the actual arrangement of the film, which accounts for the observed R3 LEED pattern. The Fourier transform (FT) of the STM images acquired on the R3 phase gives a direct proof that the $(3\sqrt{3}\times 3\sqrt{3})$ periodicity belongs to the molecular layer and not to the arrangement of the substrate atoms. The R13 phase is also analyzed with submolecular resolution STM and the orientation of the molecules in this phase is determined.

II. EXPERIMENT

After the introduction into the UHV apparatus (base pressure of 1×10^{-10} mbar), the Ge(111) wafer has been degassed for several hours at 450°C . The surface has been prepared by several cycles of sputtering with Ar^+ ions at 700 eV and series of short (about 20 s) annealing at 700°C . The quality of the surface $c(2\times 8)$ reconstruction has been checked by LEED after every preparation process. C_{60} powder has been evaporated in the same UHV conditions from a tantalum crucible by resistive heating. Before deposition, the C_{60} source has been degassed at $350\text{--}400^\circ\text{C}$ for several hours. During the evaporation, the crucible temperature, monitored by a thermocouple welded to the crucible, has been kept at about 400°C , with the pressure in the preparation chamber never exceeding 7×10^{-10} mbar. The STM measurements have been carried out *in situ* in a connected UHV chamber (base pressure of 3×10^{-11} mbar) with an Omicron Multiscan System. The STM data have been acquired in constant current mode with tip to sample biases ranging from $+2.0$ to -2.0 V. 1 ML (monolayer) is defined as the density of the single layer of C_{60} molecules left on the Ge(111) surface after annealing a C_{60} multilayer at 300°C .

III. RESULTS AND DISCUSSION

A. $(3\sqrt{3}\times 3\sqrt{3})R30^\circ$ phase

Figure 1(a) shows the LEED pattern acquired on the C_{60}

film after the deposition of about 3 ML and subsequent annealing at 450°C . The sharp spots enclosed by circles correspond to the (1×1) hexagonal periodicity of the Ge substrate. The other broader spots indicate the presence of the R3 hexagonal periodicity, whose lattice vectors are indicated by the short white arrows (the inner spots are not visible because they are hidden by the shadow of the electron gun). We recall that the R3 pattern corresponds to a periodicity of 2.04 nm in the real space. The STM image in Fig. 1(b) shows the morphology of the same system. In agreement with previous observations,¹ the molecules are arranged in a hexagonal close packed lattice with an average nearest neighbor distance of about 1.0 nm. In this STM image, the submolecular features are not resolved. Note the presence of some background in the LEED image and that the R3 spots are much broader than the ones due to the substrate, indicating that the degree of order of the surface is not high and that the R3 periodicity is extended over small domains. Accordingly, the STM image shows that the hexagonal molecular lattice of the film is defective or distorted in many points. An evaluation of the defect density averaged on several images can be given by measuring the uncovered area [observed as dark areas in Fig. 1(b)] of the film, resulting to be about 14% of the total area.

Here, we want to focus the attention onto the origin of the LEED periodicity (2.04 nm), which does not correspond to the molecule-molecule distance, as seen by STM (1.02 nm).¹ Xu *et al.*¹ explained the discrepancy between LEED and STM periodicity by considering a substrate reconstruction. In their model, the Ge(111) adatoms that in the clean surface reconstruct in the $c(2\times 8)$ lattice rearrange in a R3 lattice upon C_{60} adsorption and annealing, explaining the observed R3 LEED pattern and the disappearance of the $c(2\times 8)$ pattern. Goldoni *et al.*² proposed a different model based on core-level photoemission data. Upon the molecular adsorption and the thermal treatment, the Ge adatoms are no longer present on the surface, which rearranges in the Ge(111)- (1×1) hexagonal lattice as a bulk terminated crystal. Hence, the R3 LEED pattern is due to the alternating orientations of the molecules in the hexagonal molecular superlattice, which results in a (2×2) unit cell (defined with respect to the molecular hexagonal superlattice observed by STM,¹ where the unit vector is ~ 1.0 nm). The model is based on four different molecular orientations, corresponding to four different configurations of the substrate atoms under the molecules. The model proposed in Ref. 2 is sketched in Fig. 2, where the big circles represent, by different filling, the different adsorption sites. This model is supported by the almost complete quenching of the adatom contribution in the Ge 3d photoemission spectra,² which at the same time discards the model proposed by Xu *et al.*¹

To investigate the actual origin of the R3 periodicity and, in particular, to verify the hypothesis of alternating orientations, high resolution STM measures have been obtained, providing the observation of submolecular features. In general, this allows to determine whether two molecules have the same orientation. Furthermore, in some cases and with supporting calculations,^{15,20,23,24} the analysis of the submolecular features can lead to the recognition of the orientation

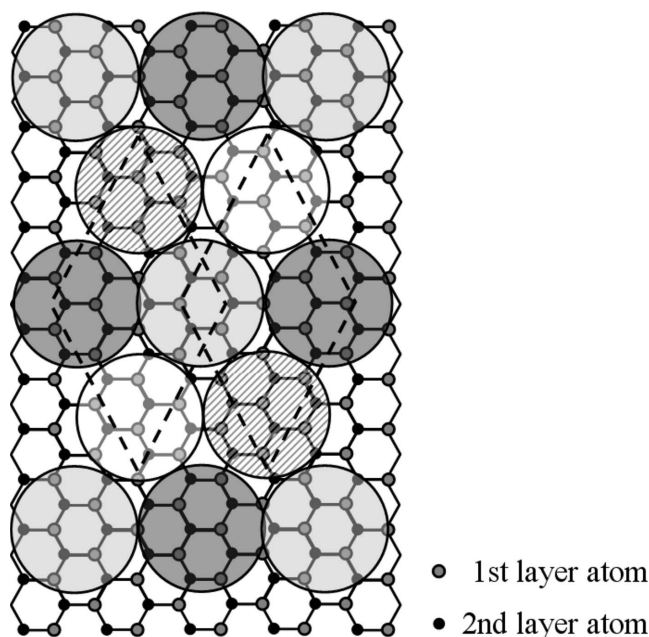


FIG. 2. Sketch of the C₆₀ adsorption sites on the Ge(111) surface in the R3 phase taken by the model of Goldoni *et al.* (Ref. 2). The big circles indicate the position of the C₆₀ molecules and the different colors indicate different adsorption sites. The meaning of the black dotted rhombus is explained in the text.

of the molecule, as for the R13 phase (see the next section).

Figure 3(a) [same scale of Fig. 1(b)] shows a STM image of the R3 system, allowing to distinguish submolecular features. At a first glance, no long-range order appears in the periodicity of the molecular orientations. The Fourier transform of Fig. 3(a) is shown in Fig. 3(b), while in Fig. 3(c), the FT of the STM image in Fig. 1(b) is shown. To enhance the contrast, the FT-STM images have been filtered at low frequencies (exponential high-pass filter, cutoff at 0.5 nm⁻¹), which produces the black circular region in the center of the images. In both images, the inner black hexagon indicates the spots yielded by the (1 × 1) periodicity of the molecular lattice. Along the outer hexagon (white dotted line), whose side is twice the one of the black hexagon, some spots are visible that belong to the second order of the (1 × 1) molecular periodicity. The spots observed in Fig. 3(b) along the hexagon in the middle (white full line) correspond to the third order of an R3 periodicity (the first order R3 spots are not visible because of the low frequency filtering mentioned above). Such spots are not observed in the FT in Fig. 3(c), which correspond to a STM image where submolecular resolution is not achieved. Hence, the presence of the R3 periodicity for Fig. 3(b) can be ascribed to a periodicity of the submolecular features. Actually, the R3 pattern in the FT-STM could also come from a substrate reconstruction induced by the molecules which would create an actual height difference between the molecules. However, in this case, the R3 pattern should also be detected in the FT in Fig. 3(c), which corresponds to a STM image acquired on the same system with lower lateral resolution, but with the same vertical resolution. Anyway, a comparison with the literature can better clarify. There are some cases in which adsorption of

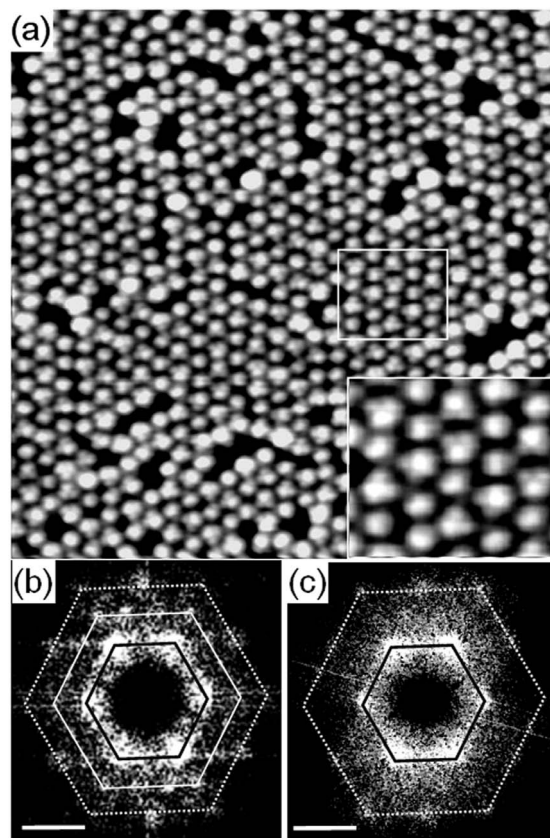


FIG. 3. (a) STM image ($25 \times 25 \text{ nm}^2$, $V=2.4 \text{ V}$, $I=1.6 \text{ nA}$) with submolecular resolution. In the inset, an area of the image (white rectangle, $5.0 \times 4.1 \text{ nm}^2$) is shown at higher magnification. (b) FT of the STM image in (a). The black and the white dotted hexagons indicate the first and second order spots of the molecular network periodicity. The white hexagon between them indicates the R3 periodicity spots (see text). The white bar at the bottom left is 1 nm^{-1} long in the reciprocal space. (c) FT of the STM image in Fig. 1(b). The FT image has been rotated and aligned with the one in (b). The symbols are as in (b).

C₆₀ actually induces a surface reconstruction (a reconstruction of the substrate induced by the adsorption of C₆₀ molecules has already been observed in several systems as reported, for example, in Refs. 4, 5, 7, and 16) which is detected in the STM images as a periodical variation in brightness, as, for example, for C₆₀ on Ag (100).¹⁶ In that case, the apparent height difference between bright and dim molecules is about 0.1–0.2 nm. In the present case the maximum apparent height difference between molecules is about 0.04 nm, with an estimated uncertainty (mainly given by noise) of 0.01 nm. Hence, we believe that it is unlikely that the R3 pattern in the FT-STM is given by a substrate reconstruction but rather comes from a true periodicity in the submolecular features pattern.

More insight on the actual origin of the R3 periodicity is obtained by analyzing high resolution STM images in more detail as in the following. In the STM image shown in Fig. 4(a), submolecular features are clearly visible. Almost all the molecules can be divided into two types: the first type, named A in Fig. 4(c), appears as a bright spot with two

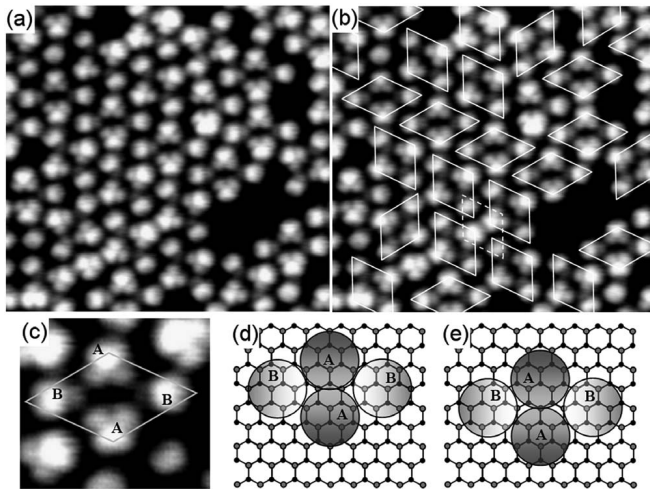


FIG. 4. (a) High resolution STM image ($10.4 \times 9.8 \text{ nm}^2$, $V=2.5 \text{ V}$, $I=1.6 \text{ nA}$) of the R3 phase. (b) Same STM image of (a) where tetramers are indicated by the white rhombus. The meaning of the dotted rhombus is explained in the text. (c) Detail ($2.9 \times 2.6 \text{ nm}^2$) of the STM image in (a). In (b) and (c), the size of the rhombus has been arbitrarily chosen, i.e., they do not correspond to the boundaries of a unit cell. [(d) and (e)] Sketch of the two possible C_{60} tetramer adsorption sites on the Ge(111) surface in the R3 phase according to the tetramer symmetry (see text). They correspond to the two tetramers indicated by the rhombus in Fig. 2 [model of Goldoni *et al.* (Ref. 2)]. The dark gray and light gray circles correspond to the A-type and B-type molecules, respectively, the shadow reflecting the symmetry of the molecules in the tetramer.

smaller lobes on one side, while the other type, named B, is almost spherical, but a slight elongation on one side is visible. The molecules in the monolayer are arranged in rhomboidal structures, each made of four molecules, hereafter named tetramers. The tetramer structure, shown in detail in Fig. 4(c), is made of two A-type and two B-type molecules. The A-type molecules are oriented with the bright spot outward, while the elongation of the B-type molecules is oriented inward. The tetramers are evidenced in Fig. 4(b) (white rhombus), where one can observe that, due to the substrate surface symmetry, three different orientations of the tetramers are present in the film, rotated each other by 60° . Small domains where tetramers are homogeneously oriented are commonly observed, up to a size of six to seven tetramers. For example, in Fig. 5, the largest domains are indicated by white lines. However, adjacent tetramers showing different orientations are frequently observed, limiting the overall domain size. The tetramer structure shown in Fig. 4(c) has not been arbitrarily chosen, but it represents the stable structure in which the molecules are arranged. In fact, by this elementary structure, it is possible to cover almost all the films, even in the proximity of defect boundaries [see Fig. 4(b)], which is not possible by choosing any other group of neighbor molecules.

Inside each domain, a (2×2) periodicity in the molecular lattice is actually present because the primitive vector with 2 nm modulus is yielded by the alternating orientation of adjacent molecules in the three equivalent directions (ori-

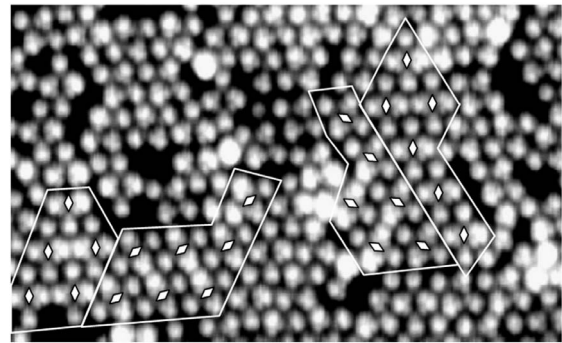


FIG. 5. STM image ($22 \times 13.4 \text{ nm}^2$, $V=2.4 \text{ V}$, $I=1.6 \text{ nA}$) of the R3 phase. White lines indicate the larger domains in the area. Within the domains, each tetramer is indicated by a white rhombus in the center.

ented 60° to each other). In such (2×2) lattice, the unit cell is the tetramer itself. Furthermore, even if different domains have a different orientation of the tetramers, the (2×2) periodicity is in the same direction since the domains also have a 60° relative orientation. Therefore, the presence of such domains where tetramers are homogeneously oriented fully accounts for the observed R3 LEED and FT-STM pattern, explaining the real structure of the R3 phase.

We now turn to discuss the physical origin of such arrangement. The observed film structure is consistent with the hypothesis that the C_{60} orientation is determined by the geometric configuration of the Ge atoms at the molecule adsorption site, as proposed by Goldoni *et al.*² In their model, four different molecular orientations are expected, depending on the Ge substrate atom configuration under each molecule (Fig. 2). Considering the symmetry of the tetramer observed by STM, it is required that the adsorption sites of the A molecules have a mirror configuration with respect to the longer diagonal. Similarly, the sites of B molecules should have a mirror configuration with respect to the shorter diagonal. In Figs. 4(d) and 4(e), the two possible tetramer adsorption sites that fulfill the symmetry requirements (considering only the first layer of atoms) are shown. They can also be recognized in the model of Goldoni *et al.* and correspond to the two dotted black rhombuses in Fig. 2. One can suppose that one of these adsorption sites belongs to the tetramer structure indicated in Fig. 4(c) and the other one to the tetramers indicated by the dotted white line in Fig. 4(b). Note that within each domain (disregarding the domain boundaries), the two tetramers can be equivalently chosen to describe the lattice and have the same symmetry. However, we recall that, considering the behavior of molecules at the domain boundaries and the defect boundaries, the tetramer in Fig. 4(c) is the only suitable building block to describe the film structure. The question about which of the two adsorption sites [Fig. 4(d) and 4(e)] is the actual one for the tetramer in Fig. 4(c) cannot be answered by means of our STM data.

It is important to stress that, in any case, the two A-type adsorption sites no longer have mirror configurations if one considers also the Ge substrate atoms of the second layer (black dots). Hence, the symmetric orientation of the A mol-

ecules within the tetramer can be regarded as an indication that only the first layer atoms are involved in the bond with C₆₀. In other words, the C₆₀ monolayer, which is formed by tetramers oriented in three equivalent directions, retains the sixfold rotational symmetry (invariant for 60° rotations) of the first layer of Ge atoms, which indicates that the interaction does not involve the second Ge layer (in this case, the symmetry should be only threefold).

Concerning the bond between the molecules and the substrate, several facts indicate that it is a strong chemical bond. First, the molecules in the R3 phase do not desorb from the substrate even at 450 °C, while the sublimation temperature of the C₆₀ crystal, where only intermolecular interactions are present, is about 230 °C in vacuum. Second, the molecules do not rotate at RT, while in the C₆₀ molecular crystal, they freely rotate at temperatures down to -40 °C at the (111) surface (and -20 °C in the bulk).²² Third, UPS valence band spectra reveal a splitting of the highest occupied molecular orbital state in two peaks at about 2.3 and 1.8 eV below Fermi level,^{2,8} which is also observed at the C₆₀/Si(111) and C₆₀/Si(100) interfaces, where a chemical bonding between some C₆₀ carbon atoms with the substrate takes place.²⁵⁻²⁷ Finally, concerning the nature of this strong bond, zero density of states at the Fermi level indicates that no partial filling of the lowest unoccupied molecular orbital (LUMO) occurs.^{2,8} This suggests the presence of a covalent bond instead of an ionic one.²¹

Summarizing, there are several factors suggesting that the orientations of the molecules are determined by the molecule-substrate interaction: (1) the bond between the molecules and the substrate is a strong covalent bond; (2) the adsorbed monolayer retains the substrate symmetry, i.e., the tetramers are oriented along the high symmetry directions of the substrate surface; (3) in agreement with the model proposed by Goldoni *et al.*,² the internal symmetry of submolecular features within the tetramers mimics the symmetry of the underlying substrate.

However, there are some clues that suggest a possible role of the intermolecular interactions. (1) Almost all the molecules (about 95%) are organized in a tetramer, as shown in Fig. 4(c), i.e., there are a very small number of isolated molecules or incomplete tetramers, also in the proximity of (2×2) domain boundaries or uncovered areas. This means that, from an energetic point of view, it is favorable for a molecule to join a tetramer up to the completion of it, i.e., complete tetramers are more stable than incomplete ones, and this additional gain in energy should be related to intermolecular interactions. (2) The distance between the molecules is ~1 nm, which is the equilibrium distance for the van der Waals intermolecular interaction, i.e., the distance observed in the (111) plane of the C₆₀ molecular crystal. At this distance, van der Waals and Coulombic interactions are not negligible and strong enough to determine the molecular orientation (at low temperature) in systems where no other strong interactions are present, as, for example, in the (111) surface of C₆₀ crystal (below 230 K, see Ref. 28 and references therein), in the C₆₀ monolayer on graphite (observed at 100 K),²⁹ and on the C₆₀ monolayer on an inert self-assembled monolayer (SAM) (observed at 5 K).^{19,20} Note that for the C₆₀ (111) plane and C₆₀ monolayer on SAM, a

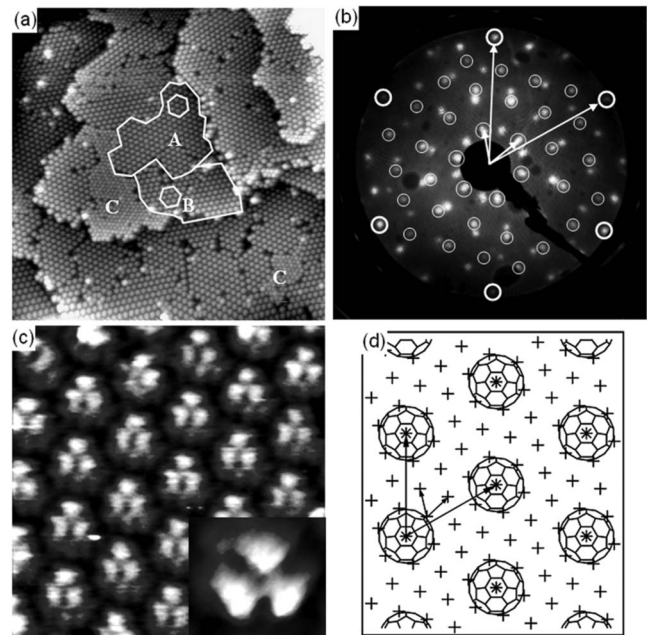


FIG. 6. (a) STM image ($80 \times 80 \text{ nm}^2$, $V = -2.0 \text{ V}$, $I = 1.8 \text{ nA}$) of the C₆₀/Ge film in the R13 phase (after annealing at 550 °C). The white lines indicate two differently oriented domains, labeled A and B. The C label indicates residual R3 domains. (b) R13 LEED pattern ($E_p = 23 \text{ eV}$) acquired on the same system of (a), which is the sum of two hexagonal reciprocal lattices. One of them is indicated by smaller circles, the short arrows being its reciprocal unit vectors. Bold circles indicate the spots of the (1×1) periodicity of the substrate, the long arrows being its reciprocal unit vectors. (c) High resolution STM image ($7.4 \times 7.4 \text{ nm}^2$, 2.0 V, 1.8 nA) in which the molecular orbitals are visible. In the inset, single molecule STM image detail is shown. (d) Sketch of the arrangement of the molecules with respect to the (1×1) substrate lattice (black crosses) as deduced by LEED and STM.

(2×2) periodicity in the molecular superlattice due to the alternating orientation has also been observed, but in these cases, the orientation of the molecules is completely different from what observed here.^{19,28} (3) Finally, we would remark the result reported in Ref. 18 about C₆₀/Cu(110), where it is shown that the intermolecular interactions play a role in the orientation of the molecule even though a strong interaction with the substrate is present similarly to our system.

In conclusion, we have shown that the real structure of the R3 phase is made by the tetramers. We believe that the orientation of the molecules in the tetramer is mostly determined by the interaction with the substrate, as suggested by Goldoni *et al.*² On the other hand, a secondary contribution to the resulting tetramer structure from the intermolecular interactions should be taken into account. This point could be further clarified by knowing the exact orientation of A-type and B-type molecules, which would be possible by comparing STM data with theoretical calculations.

B. ($\sqrt{13} \times \sqrt{13}$)R14° phase

In Fig. 6(a), the STM image of the C₆₀/Ge film is shown after an annealing treatment of 10 min at 550 °C. In agree-

ment with literature,¹ the molecules are arranged in a hexagonal lattice with an average distance between molecules of 1.4 ± 0.1 nm. There are two equivalent domains, two of them are indicated in Fig. 6(a) by A and B, rotated by 28° apart. Moreover, some residual R3 domains are still present in the film, indicated by C, suggesting that the transition to the R13 phase is not yet complete. In Fig. 6(b), the corresponding LEED pattern is shown. Accordingly with that reported in Refs. 1 and 8, the LEED indicates an R13 superlattice unit cell. The LEED pattern is the superposition of two hexagonal lattices rotated by 14° with respect to the $\text{Ge}(1 \times 1)$ hexagonal lattice [the circles in Fig. 6(b) indicate one of the two hexagonal patterns], which correspond to the two domains observed in the STM image. The presence of the two domains, which are specular with respect to the high symmetry directions of the substrate hexagonal lattice, is expected since the 14° tilt breaks the reflection symmetry along the same directions. The spots of the diffraction pattern are sharper than the ones observed on the R3 phase, in agreement with the high degree of order observed by STM.

Figure 6(c) shows a high resolution STM image, where the submolecular features are visible. In particular, in a single domain, every molecule has the same trilobate shape [inset of Fig. 6(c)] and the same orientation, forming a lattice invariant for 120° rotations. A comparison with literature allows to determine the actual adsorption configuration of the molecule. With the sample at positive bias, the STM image shows the LUMO real space charge distribution, which is centered on the C-C bonds between a hexagon and a pentagon.^{15,23} Therefore, at a sample bias of +2.0 V, the bright features correspond to the pentagons, as confirmed also by STM image simulations reported in Ref. 15. As a consequence, the observed features indicate that the molecules adsorb with a hexagon facing up, which is the darker region in the center of the three bright lobes. The same orientation has been deduced from the same trilobate STM shape in Ref. 30.

Within the resolution of the data, the molecule results to be azimuthally aligned along the high symmetry directions of the molecular lattice, i.e., the three bright lobes, which correspond to the pentagons, point toward the neighbor molecules [see Fig. 6(d)].

In the domains of the same type, A or B, the orientation of the molecules is univocally determined. In other words, in our data, we do not observe molecules in the same domain, or in two homogeneously oriented domains, with two equivalent orientations tilted by 60° . On the contrary, this should be expected in the case of a substrate with sixfold rotational symmetry (see, for example, Ref. 30). For this reason, we believe that the second layer atoms are also involved in the interaction between the molecule and the substrate. In fact, in this case, the symmetry of the substrate is threefold and not sixfold, as for the first layer only. The present STM data cannot indicate what the actual adsorption site of the molecules is. Torrelles *et al.*³¹ studied the system by means of grazing incidence x-ray diffraction and suggest that the substrate reconstructs, forming pits (i.e., holes with ~ 1 nm diameter) by removing atoms of the first two layers. C_{60} are hosted in these holes, forming covalent bonds with the surrounding atoms.³¹ Their model is in perfect agreement

with our STM data, including the orientation of the molecules.

Thermally activated phases of C_{60} monolayer have been already observed where a reconstruction of the substrate takes place in order to host the molecules: $\text{C}_{60}/\text{Au}(110)-p(6 \times 5)$,³² $\text{C}_{60}/\text{Al}(111)(6 \times 6)$,³³ and different phases of $\text{C}_{60}/\text{Pd}(110)$ (Ref. 34) and $\text{C}_{60}/\text{Pt}(111)$.^{35,36} In the latter, a $(\sqrt{13} \times \sqrt{13})R14^\circ$ molecular superlattice is observed as well as in the present system (but with a molecule-molecule distance of 1.0 nm) and the orientation of the molecule with a hexagon facing up is also observed. In all of these systems, the bond between the molecule and the substrate is considered to be covalent.

Concerning the interaction between molecules and substrate, it is believed that there is a covalent bond as well in the R3 phase. This is in accordance with the strength of the bond (desorption takes place at 670°C , Ref. 8) and with the absence of partially filled LUMO in the UPS spectra, which excludes the possibility of an ionic bond.⁸ While for the R3 phase the interaction between molecules can have some role in determining the resulting structure and the orientation of the molecules, in the case of R13, the long distance between neighbors would suggest that the intermolecular forces can be safely neglected. Moreover, calculations show that the interaction potential between the C_{60} molecules with a center-center distance of 1.4 nm is very close to zero (Ref. 37 and references therein). However, there are two hints that raise the question about a possible role of the intermolecular interactions. (1) It is remarkable that the molecules, within our STM measurement resolution, are azimuthally oriented along the high symmetry direction of the molecular lattice and not symmetric with respect to the substrate. This is also in agreement with that reported in Ref. 31. Actually, considering the strong interaction with the substrate and the large distance between the molecules, one should expect the molecules to be azimuthally aligned with the substrate, according to the symmetry of the adsorption site, as it happens, for example, in the $\text{C}_{60}/\text{Pt}(111)-(\sqrt{13} \times \sqrt{13})R14^\circ$ monolayer, where molecules are 1.0 nm apart.^{35,36} (2) In the observed arrangement, neighbor molecules face each other, conjugating region poor of charge (hexagon-hexagon bonds) with region rich of charge (pentagons). This arrangement, in principle, is the one which minimizes the interaction potential. Therefore, even in this case, the present information cannot exclude a role of the intermolecular interactions over the system geometric arrangement.

IV. CONCLUSIONS

High resolution STM measurements have shown that the unit cell of a monolayer of C_{60} molecules in the R3 phase on the $\text{Ge}(111)$ surface is made of tetramers. The tetramers can be oriented along three equivalent directions. Domains of homogeneously oriented tetramers are observed, accounting for the R3 pattern observed by LEED. The observed structure of the film is in agreement with the hypothesis that the orientation of the molecules is mostly determined by the configuration of the first layer Ge atoms. However, some clues indicate that the interaction between adjacent molecules,

even though weaker than the strong covalent bond between C₆₀ and the substrate, have probably an ancillary role in the resulting arrangement.

High resolution STM data have also shown that the molecules in the R13 phase are homogeneously oriented within each of the two observed domains. The submolecular STM features indicate that the molecules are bonded with a hexagon facing the substrate. The threefold symmetry of the domains suggests that the Ge substrate atoms of the second layer are also involved in the bonding. A comparison with literature suggests that the substrate undergoes to a reconstruction forming pits where molecules are hosted. In this

case, the orientation of the molecules can be ascribed to the interaction with the substrate, even if there are some clues that do not allow to completely exclude a role of intermolecular interactions.

ACKNOWLEDGMENTS

The nanospectroscopy facility in Brescia was funded by INFN under the “Strumentazione Avanzata” programme. This work has been partially funded by “FIRB Carbon-based microstructures and nanostructures” programme of MIUR.

- ¹H. Xu, D. M. Chen, and W. N. Creager, *Phys. Rev. B* **50**, 8454 (1994).
- ²A. Goldoni, C. Cepek, M. De Seta, J. Avila, M. C. Asensio, and M. Sancrotti, *Phys. Rev. B* **61**, 10411 (2000).
- ³J. C. Dunphy, D. Klyachko, H. Xu, and D. M. Chen, *Surf. Sci.* **383**, L760 (1997).
- ⁴K. R. Wirth and J. Zegehnagen, *Phys. Rev. B* **56**, 9864 (1997).
- ⁵K. R. Wirth and J. Zegehnagen, *Surf. Sci.* **351**, 13 (1996).
- ⁶D. V. Klyachko, J.-M. Lopez-Castillo, J.-P. Jay-Gerin, and D. M. Chen, *Phys. Rev. B* **60**, 9026 (1999).
- ⁷T. Kidd, R. D. Aburano, H. Hong, T. Gog, and T.-C. Chiang, *Surf. Sci.* **397**, 185 (1998).
- ⁸G. Bertoni, C. Cepek, and M. Sancrotti, *Appl. Surf. Sci.* **212-213**, 52 (2003).
- ⁹J. G. Hou, Y. Jinlong, W. Haiqian, L. Qunxiang, Z. Changgan, L. Hai, B. Wang, D. M. Chen, and Z. Qingshi, *Phys. Rev. Lett.* **83**, 3001 (1999).
- ¹⁰J. I. Pascual, J. Gómez-Herrero, C. Rogero, A. M. Baró, D. Sanchez-Portal, E. Artacho, P. Ordejón, and J. M. Soler, *Chem. Phys. Lett.* **321**, 78 (2000).
- ¹¹C. Zhou, J. Wu, B. Han, S. Yao, and H. Cheng, *Phys. Rev. B* **73**, 195324 (2006).
- ¹²W. L. Yang, V. Brouet, X. J. Zhou, H. J. Choi, S. G. Louie, M. L. Cohen, S. A. Kellar, P. V. Bogdanov, A. Lanzara, A. Goldoni, F. Parmigiani, Z. Hussain, and Z.-X. Shen, *Science* **300**, 303 (2003).
- ¹³V. Brouet, W. L. Yang, X. J. Zhou, H. J. Choi, S. G. Louie, M. L. Cohen, A. Goldoni, F. Parmigiani, Z. Hussain, and Z. X. Shen, *Phys. Rev. Lett.* **93**, 197601 (2004).
- ¹⁴A. Tamai, A. P. Seitsonen, R. Fasel, Z. X. Shen, J. Osterwalder, and T. Greber, *Phys. Rev. B* **72**, 085421 (2005).
- ¹⁵L.-L. Wang and H.-P. Cheng, *Phys. Rev. B* **69**, 165417 (2004).
- ¹⁶C.-L. Hsu and W. W. Pai, *Phys. Rev. B* **68**, 245414 (2003).
- ¹⁷R. Fasel, P. Aebi, R. G. Agostino, D. Naumovic, J. Osterwalder, A. Santaniello, and L. Schlapbach, *Phys. Rev. Lett.* **76**, 4733 (1996).
- ¹⁸R. Fasel, R. G. Agostino, P. Aebi, and L. Schlapbach, *Phys. Rev. B* **60**, 4517 (1999).
- ¹⁹L.-F. Yuan, J. Yang, H. Wang, C. Zeng, Q. Li, B. Wang, J. G. Hou, Q. Zhu, and D. M. Chen, *J. Am. Chem. Soc.* **125**, 169 (2003).
- ²⁰J. G. Hou, Y. Jinlong, W. Haiqian, L. Qunxiang, Z. Changgan, Y. Lanfeng, W. Bing, D. M. Chen, and Z. Qingshi, *Nature (London)* **409**, 304 (2001).
- ²¹A. J. Maxwell, P. A. Brühwiler, D. Arvanitis, J. Hasselström, M. K.-J. Johansson, and N. Mårtensson, *Phys. Rev. B* **57**, 7312 (1998).
- ²²R. Blinc, J. Seliger, J. Dolinšek, and D. Arčon, *Phys. Rev. B* **49**, 4993 (1994).
- ²³J. I. Pascual, J. Gomez-Herrero, D. Sanchez-Portal, and H.-P. Rust, *J. Chem. Phys.* **117**, 9531 (2002).
- ²⁴Y. Maruyama, K. Ohno, and Y. Kawazoe, *Phys. Rev. B* **52**, 2070 (1995).
- ²⁵S. Suto, K. Sakamoto, D. Kondo, T. Wakita, A. Kimura, A. Kakizaki, C.-W. Hu, and A. Kasuya, *Surf. Sci.* **438**, 242 (1999).
- ²⁶M. De Seta, D. Sanvitto, and F. Evangelisti, *Phys. Rev. B* **59**, 9878 (1999).
- ²⁷C. Cepek, P. Schiavuta, M. Sancrotti, and M. Pedio, *Phys. Rev. B* **60**, 2068 (1999).
- ²⁸H. Wang, C. Zeng, B. Wang, J. G. Hou, Q. Li, and J. Yang, *Phys. Rev. B* **63**, 085417 (2001).
- ²⁹Z. Y. Li, *Surf. Sci.* **441**, 366 (1999).
- ³⁰T. Hashizume, K. Motai, X. D. Wang, H. Shinohara, Y. Saito, Y. Maruyama, K. Ohno, Y. Kawazoe, Y. Nishina, H. W. Pickering, Y. Kuk, and T. Sakurai, *Phys. Rev. Lett.* **71**, 2959 (1993).
- ³¹X. Torrelles, T. L. Lee, O. Bikondoa, J. Rius, and J. Zegehnagen, in *ESRF Highlights 2003*, edited by G. Admans (unpublished), p. 75.
- ³²M. Pedio, R. Felici, X. Torrelles, P. Rudolf, M. Capozzi, J. Rius, and S. Ferrer, *Phys. Rev. Lett.* **85**, 1040 (2000).
- ³³M. Stengel, A. De Vita, and A. Baldereschi, *Phys. Rev. Lett.* **91**, 166101 (2003).
- ³⁴J. Weckesser, J. V. Barth, and K. Kern, *Phys. Rev. B* **64**, 161403(R) 2001.
- ³⁵R. Felici, M. Pedio, F. Borgatti, S. Iannotta, M. Capozzi, G. Ciullo, and A. Stierle, *Nat. Mater.* **4**, 688 (2005).
- ³⁶L. Giovanelli, C. Cepek, L. Floreano, E. Magnano, M. Sancrotti, R. Gotter, A. Morgante, A. Verdini, A. Pesci, L. Ferrari, and M. Pedio, *Appl. Surf. Sci.* **212-213**, 57 (2003).
- ³⁷D. Klyachko and D. M. Chen, *Phys. Rev. Lett.* **75**, 3693 (1995).